Saikrishna *et al.*
Protection and Control of Modern Power Systems (2022) 7:14
https://doi.org/10.1186/s41601-022-00235-0

Protection and Control of Modern Power Systems

ORIGINAL RESEARCH Open Access

Adaptive relay co-ordination using a busbar splitting approach for a system integrity protection scheme

Rajesh Saikrishna*, Nilesh Kumar Rajalwal and Debomita Ghosh

Abstract

Power system faults can often result in excessively high currents. If sustained for a long time, such high currents can damage system equipment. Thus, it is desirable to operate the relays in the minimum possible time. In this paper, a busbar splitting approach is used for adaptive relay setting and co-ordination purposes for a system integrity protection scheme (SIPS). Whenever a fault occurs, the busbar splitting scheme splits a bus to convert a loop into a radial structure. The splitting schemes are chosen such that the net fault current is also reduced. Busbar splitting eliminates the dependency upon minimum breakpoints set (MBPS) and reduces the relay operating time, thus making it adaptive. The proposed methodology is incorporated into the IEEE 14-bus and IEEE 30-bus systems with single and multiple fault conditions. The modeling and simulation carried out in ETAP, and the results of the proposed busbar splitting-based relay co-ordination are compared with the MBPS splitting-based relay co-ordination.

Keyword: System integrity protection scheme (SIPS), Relay co-ordination, Minimum breakpoint set (MBPS), Ward equivalent method, Busbar splitting, Wide area monitoring system (WAMS), ETAP

1 Introduction

Power system networks are prone to electrical faults which may occur for numerous reasons such as lightning, equipment failure, or other environmental reasons. High fault current is the ultimate consequence, irrespective of the type of electrical fault. Hence, protecting the power system network is of utmost concern and to be achieved by making sure that faults are cleared in the minimum possible time. Modern technologies such as the wide area monitoring system (WAMS), and using phasor measurement units (PMU), have led to the gradual development of system integrity protection schemes (SIPS), which oversee the complete network and undertake necessary actions to prevent system blackout.

Reference [1] describes the architecture of SIPS and its application in the power industry, while information from industrial engineering and research prospects is also included. In [2], a detailed literature review on the classification, purpose, implementation methods, and application of SIPS is presented, and the application of SIPS for improving system stability, avoiding distance relay mal-operation, reducing load shedding, etc. is briefly discussed. In [3], SIPS is used to avoid unwanted tripping of relays and prevent cascaded tripping which could result in system collapse. Two different algorithms are used to achieve this objective, i.e., changing the relay characteristics and identifying various points in the system, so as to help avoid relay mal-operation. In [4], a special protection scheme is proposed which depends on the various readings and measurements that are provided by the power system characteristics and the measurements from SCADA to protect the Kinmen power system from collapsing. A prevention scheme is proposed in [5] by analyzing and taking predetermined actions after severe disturbance conditions. In [6], an indices-based scheme is proposed to avoid the mal-operation of the distance relay, and synchronized data is used for the calculation of the

*Correspondence: rajeshsaikrishnapati@gmail.com
Birla Institute of Technology, Mesra, Ranchi, India

proposed indices. Reference [7] develops a methodology that identifies the fault location and the bus in the nearest vicinity using PMU-based wide area protection. In [8], a technique based on WAMS is proposed to identify the faulty equipment in the protection system, in which the status signals from the circuit breakers, the voltage and current phasors, and decisions from relays, are used to find the faulty equipment. In [9], a methodology for the enhancement of SIPS is proposed that includes enhancement of its architecture by an algorithm involving the optimal power flow of the AC and DC. The requirement for testing the SIPS and its architecture before installing in the field is also provided. In [10], a method is proposed to overcome the challenges seen by SIPS because of high penetration of renewable energy and stressed conditions that lead to relay maloperation. The proposed method is classified into two techniques, with the first technique based on the security index of the relay to achieve a faster operation of zone 3 and the second technique based upon the stability index to foresee the conditions of system stability and take corrective action.

A model-based approach for calculating the fault location is proposed in [11], one that uses control and processing software, along with simulation results of the power system. The proposed method overcomes the limitation of fault location calculation based on impedance. In [12], a methodology to find the fault location in an AC meshed microgrid is proposed, in which the fault location is identified by using support vector machines (SVM). Reference [13] proposes a mechanism to improve the zone 3 protection of the distance relay, where PMU data is used to develop an index that is derived from the rate of change of active power. In [14], a methodology is proposed that makes use of PMU data to form an index relating to the critical clearing angle for the transient stability analysis. An integrated early warning system is proposed in [15] to detect any kind of voltage instability in the system. By extrapolating trends, the violations of limits in the reactive powers of generators and the busbar voltages can be estimated to prevent the system from breakdown.

The difficulty in clearing a fault increases with the increase in the complexity of the network. In a multi-loop transmission system, fault clearing depends heavily upon the MBPS of relays. The MBPS are those sets of relays that can cut a network in both anti-clockwise and clockwise directions [16]. In a multi-loop system, the relays which are common to more than one loop have different sets of relay settings [17]. Hence, to have a common setting for such relays, relay co-ordination starts from MBPS points. In [16], a methodology is proposed to find the MBPS using graph theory and processes such as the formation of a branch incidence matrix. The methodology is incorporated in the IEEE-14 bus system to find its breakpoints. The results of an MBPS-based relay coordination method are better and comparable with the other methods of relay coordination. In [18, 19], an algorithm is proposed to find the breakpoints using integer linear programming and a graph theory approach that considers the cardinality of a relation as the breakpoints, whereas in [20], a new methodology is proposed to identify the MBPS-based upon the power quality and the zones which are at risk of cascaded tripping. In [21], a depth-first search algorithm is proposed to determine the MBPS of the given multi-loop network. Determination of the MBPS is a time-consuming process along with the concern that different methodologies give a distinct set of results for a single network. For example, for the same network, the methods used in [16] and [19] give 10 and 9 relays as a set of minimum breakpoints, respectively. Hence, the need arises for either eliminating the requirement of MBPS or at least minimizing its use to a great extent. Also, even if the MBPS is determined for a multi-loop system, to achieve the optimum relay settings for a coordination purpose, a large number of iterations are needed.

The relay setting mainly depends upon the maximum fault current and pick-up current of a relay (which in return depends on the minimum fault current value). Hence, to have a relay setting that can reduce the fault clearing time, it is necessary to modify the maximum and minimum fault current values. In [22], superconducting fault current limiters (SFCL) are proposed to limit the level of the fault current, though in the event of SFCL failure, the fault current will not be limited. In [23], a series reactor is used to limit the fault current and act as a compensating agent, although the methodology proposed increases the impedance of the lines and affects the voltage profile in normal scenarios. Devices such as IS-limiter, or a solid-state based fault current limiter [24–26], can be used to restrict the fault current. However, all the available techniques use external devices to manage the fault current level, and in the case where they are damaged, it may lead to severe maloperation of the protection system.

In addition, power system transmission networks are too complex to be able to analyze the effects of changes within the network. References [27, 28] propose methodologies to determine the exact reduced equivalent networks to effectively examine the possible effects of events occurring in the original network. In [29], sensitivity analysis and busbar splitting techniques are used to maintain the voltage profile of the network, while such busbar splitting techniques are also used in [30, 31] for managing the islanding processes, line overloading, and

violation in voltage levels, and in [32, 33] for managing the fault current level.

This paper proposes a busbar splitting technique that clears a fault in a reduced time compared to the conventional MBPS-based relay co-ordination. It does this by minimizing the dependency on MBPS, thereby enhancing the protection objective of SIPS. The remainder of the paper is organized as follows. Section 2 details conventional MBPS-based relay co-ordination, whereas Sect. 3 describes the busbar splitting technique. In Sect. 4, the busbar splitting methodology for adaptive relay co-ordination is implemented. Section 5 gives the results and comparative analysis of the proposed and conventional techniques of relay co-ordination and Sect. 6 draws conclusions and reflects on future perspectives.

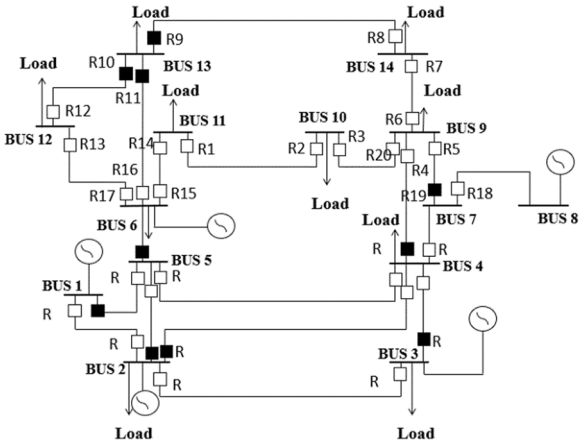

Fig. 1 MBPS of IEEE 14-bus system

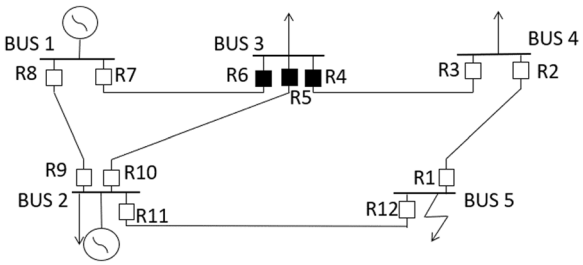

Fig. 2 5-bus system

2 MBPS-based relay co-ordination

2.1 MBPS determination

To determine the minimum breakpoint set of any given network the following steps are conducted as given in [16].

A power system network $A = (V, E)$ is considered which has m buses and n branches, with V being the set of buses given by $\{v_1, v_{2,} v_{3,} \ldots, v_m\}$ and E denoting the set of branches given by $\{e_1, e_{2,} e_{3,} \ldots, e_n\}$.

Step 1: The bus to branch admittance matrix A is formed by assigning the matrix elements (y_{ij}) as:

$+1$ when bus v_j is the starting point of branch e_i.

-1 when bus v_j is the ending point of branch e_i.

0 when bus v_j is neither the starting nor the ending point of branch e_i

Step 2: The rows of matrix A that correspond to the parallel branches in the given network are combined to obtain a reduced branch admittance matrix $\tilde{A}$, such that $\tilde{A} \in R^{n \times m}$.

Step 3: The rows of $\tilde{A}$ that are combined are permuted to the bottom of the matrix.

Step 4: The columns of $\tilde{A}$ are arranged in ascending order of their respective 2-norms.

Step 5: LU-factorization of $\tilde{A}$ is performed and terminates after r steps, where r is the rank of $\tilde{A}$ in order to determine the lower trapezoidal matrix, L, and upper trapezoidal matrix, U.

Step 6: The non-zero elements of U are used to sectionalize the given network into $m - r$ number of connected graphs.

Step 7: Considering that the *qth* connected part of the network has $\widetilde{m_q}$ buses and $\widetilde{n_q}$ branches, a reduced matrix of L is determined, one that gives $\tilde{L}$ such that $\widetilde{L} \in R^{\widetilde{n_q} \times \widetilde{m_q}}$. In $\tilde{L}$, the column consisting of the maximum number of non-zero elements in the last $\widetilde{n_q} + \widetilde{m_q} - 1$ rows is determined. Considering all the non-zero elements in the chosen column, if the non-zero element is 1, the start of the branch corresponding to the element is chosen as a break point, whereas the end is chosen as a break point if the non-zero element is -1. In the case where the non-zero matrix elements correspond to the rows of combined branches, the starts of both branches are chosen as break points, if the element is 1, whereas if the element is -1, the ends of the parallel branches are considered to be the break points. The step is repeated untill there exists at least a single non-zero element in the chosen column.

Step 8: The steps above are repeated for all the connected networks with the MBPS being the combination of the MBPS of all connected graphs.

The above-mentioned steps are implemented in the IEEE 14-bus system to determine its minimum breakpoint set [16]. Figure 1 shows the MBPS of the IEEE 14-bus system.

The relays marked in black are the MBPS for the IEEE -14 bus system. In a power network with defined MBPS, relay co-ordination always starts from the breakpoints even for particular fault conditions.

2.2 Relay co-ordination with MBPS

A 5- bus test system is considered as shown in Fig. 2, with blackened relays depicting the breakpoints. These

breakpoints are determined by implementing the steps discussed in Sect. 2.1, for a fault at bus 5.

In this case, the co-ordination of relays starts from the breakpoint relays R4, R5, and R6 simultaneously, instead of relay R1 that is nearer to the fault. This makes the TMS of relay R1 more than those of relays R4, R5, and R6 respectively. Consequently, it makes the relay operating time t_{op} long, which would otherwise have been shorter if relay R1 had operated first. The relays used in this work are assumed to have IEC standard inverse characteristics given in [17] as:

$$t_{op} = TMS_j \times \frac{0.14}{\left(\frac{I_{FMAX}}{I_S}\right)^{0.02} - 1} \tag{1}$$

where TMS_j is the time multiplier setting of relay 'j', I_{FMAX} and I_S are the maximum fault current and the pick-up value of current seen by the relay, respectively. As the pick-up value varies between the range of maximum load current to $2/3$ of the minimum fault current [17], its value used in this work for co-ordination purpose is $2/3$ of the minimum fault current. This refers to the worst-case analysis. Also, the co-ordination time interval (CTI) between the operation of two consecutive relays is considered to be 0.3 s. Knowing the fault currents seen by each relay, the TMS and t_{op} for each relay can be obtained as in [17] using (1).

3 Busbar splitting-based relay co-ordination

Busbar splitting schemes are created by the use of Ward's equivalent method for network reduction. It works by transforming a star network into an exact equivalent reduced meshed network, such that any analysis carried out in the reduced equivalent model applies to the original network. According to Ward's equivalent method [27], the transformation proceeds by eliminating the desired buses and then the boundary buses are interconnected with each other by lines having impedance given as:

$$Z_{ab} = Z_a Z_b \left(\frac{1}{Z_1} + \frac{1}{Z_2} + \frac{1}{Z_3} + \cdots + \frac{1}{Z_n}\right) \tag{2}$$

where Z_{ab} is the impedance between buses a and b, $Z_a, Z_b, Z_1, Z_2 \ldots$ are the impedances between the bus and the neutral. The buses connected directly to the bus under consideration are known as boundary buses and the rest are considered as external buses. With Q representing the boundary buses and R representing the external buses, the voltage equation of a power system network can be given as:

$$\begin{bmatrix} Y_{PP} & Y_{PQ} & Y_{PR} \\ Y_{QP} & Y_{QQ} & Y_{QR} \\ Y_{RP} & Y_{RQ} & Y_{RR} \end{bmatrix} \begin{bmatrix} V_P \\ V_Q \\ V_R \end{bmatrix} = \begin{bmatrix} I_P \\ I_Q \\ I_R \end{bmatrix} \tag{3}$$

In the case where bus P is considered to be eliminated to reduce the network, using the Gauss elimination technique, the equivalent boundary bus admittance matrix and impedance matrix are respectively given as:

$$\widehat{Y_{QQ}} = \left(Y_{QQ} - Y_{QP} Y_{PP}^{-1} Y_{PQ}\right) \tag{4}$$

$$\widehat{Z_{QQ}} = \widehat{Y_{QQ}}^{-1} \tag{5}$$

Splitting the busbar P into bus P and P', and applying the same technique as above, the after splitting equivalent admittance matrix and impedance matrix are respectively given as:

$$\widehat{Y_{QQ}}^{*} = Y_{QQ} - \begin{bmatrix} Y_{QP}^{*} & 0 \\ 0 & Y_{QP'}^{*} \end{bmatrix} \begin{bmatrix} Y_{PP}^{*} & 0 \\ 0 & Y_{P'P'}^{*} \end{bmatrix}^{-1} \begin{bmatrix} Y_{PQ}^{*} & 0 \\ 0 & Y_{P'Q}^{*} \end{bmatrix} \tag{6}$$

$$\widehat{Z_{QQ}}^{*} = \widehat{Y_{QQ}}^{*-1} \tag{7}$$

Comparing (5) and (7), the boundary bus whose impedance is increased can be found when bus P is split into buses P and P' [34], i.e., it will give the information regarding which boundary bus should be split in order to have an increased impedance at the faulty bus. The flowchart in Fig. 3 depicts the sequence in which the steps need to be followed for assessment.

Hence, in the case of a fault at one of the buses, splitting the boundary bus will result in an increase in the impedance and reduction in the fault current [34]. This change in the fault current along with the busbar splitting results in better adaptability of the network for relay co-ordination with reduced relay operating time.

4 Adaptive relay co-ordination incorporating busbar splitting

4.1 Effect of busbar splitting on relay co-ordination

Considering the example network in Fig. 2 and assuming a fault at bus 5, bus 2 is split according to the proposed scheme as shown in Fig. 4.

With the splitting of bus 2, bus 5 is no longer a part of any loop and thus makes the faulty bus radial. With relays R11 and R12 seeing no fault current, relay R1 behaves as the primary relay and hence has the least TMS as co-ordination of relays now starts from relay R1. This results in reduced fault clearing time, which otherwise would have been longer in the case where the primary relays were relay R4, R5, and R6, as in the case before splitting.

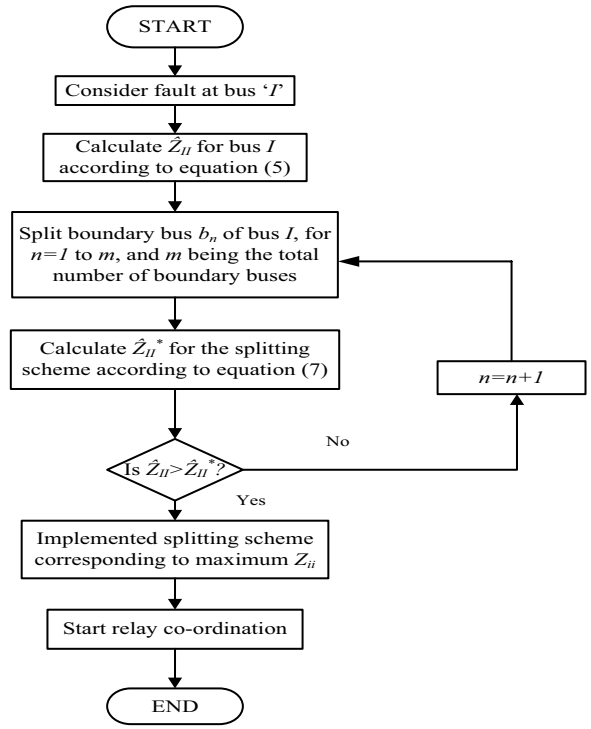

Fig. 3 Flowchart of the proposed methodology for busbar splitting

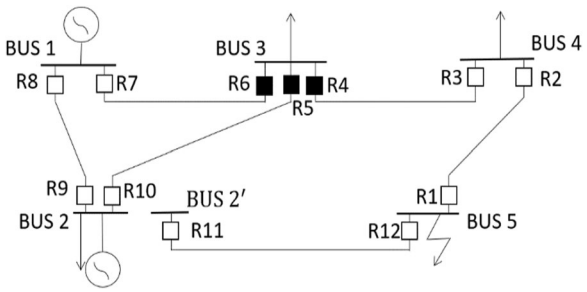

Fig. 4 5-bus system with busbar splitting scheme

4.2 Effect of fault current modification on relay operating time

From (1), it is clear that t_{op} depends upon the ratio of (I_{FMAX}/I_s). If the ratio increases, t_{op} reduces. Even if the net fault current at a bus decreases after busbar splitting, there is the possibility that the fault current seen by the relay nearest to the fault location increases. Thus along with minimizing the TMS for the relay nearest to fault location, if the ratio of (I_{FMAX}/I_s) is increased, there will be a significant dip in the operating time of the relay that is nearest to the fault. Thus, the methodology that has been described for SIPS reduces the fault clearing time.

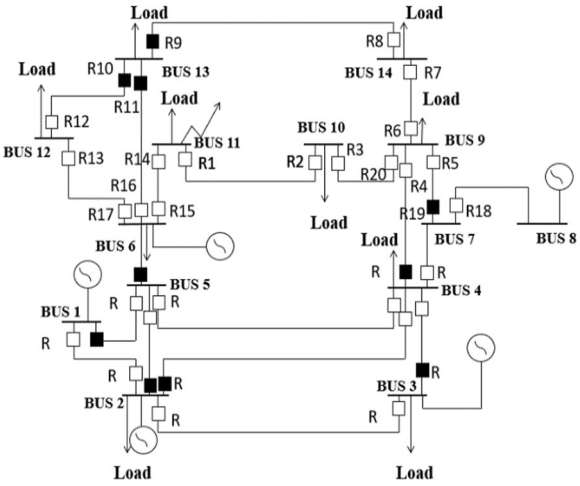

Fig. 5 IEEE 14-bus system with MBPS and fault location

Table 1 TMS and t_{op} of the nearest relay to fault and back-up relay

Faulty bus	Relay nearest to fault	t_{op} of nearest relay (s)	Backup of nearest relay	t_{op} of backup relay (s)
11	R1	1.5943	R15	1.846
	R14	0.9950	R2	1.2959

5 Results and discussion

5.1 Relay co-ordination in the IEEE 14-bus system with MBPS

The location of breakpoints for the IEEE 14-bus system and the fault location considered are shown in Fig. 5. For relay co-ordination, it is considered that bus 11 is under fault. The TMS and t_{op} for all the relays are calculated using (1) with the initial assumption of TMS = 0.025 for breakpoint relays and CTI of 0.3 s. Table 1 shows the operating time of the relays nearest to the fault and their backup relays, before incorporating splitting scheme.

5.1.1 Managing fault level with busbar splitting in the IEEE 14-bus system

Since the relay parameters such as TMS and t_{op} depend upon the fault level, it is necessary to modify the maximum and minimum fault current so t_{op} can be reduced, as given in Sect. 4.2. Table 2 shows the results of the applied busbar spitting methodology to the IEEE 14-bus system, where all the buses have been considered under fault with one bus at a time, with all possible splitting scenarios resulting in reduction in fault currents.

Table 2 Maximum and minimum fault currents under different splitting scenarios for varying fault conditions in the IEEE 14-bus system

Faulty bus	Network configuration	Splitting scenarios	Max. fault current (kA)	Min. fault current (kA)
11	Before splitting	Normal	20.691	19.965
	Splitting bus 6	6→5,11 6′→12,13, L	20.578	19.864
		6→11 6′→5,12,13, L, G	10.3	8.462
	Splitting bus 10	10→11 10′→9, L	13.528	13.089
10	Before splitting	Normal	26.871	20.735
	Splitting bus 11	11→10 11′→6, L	18.813	14.503
	Splitting bus 9	9→10 9′→4,7,14, L	10.312	7.912
9	Before splitting	Normal	35.13	25.602
	Splitting bus 10	10→9 10′→11, L	27.737	20.895
	Splitting bus 14	14→9 14′→13, L	30.376	22.755
	Splitting bus 7	7→9 7′→4,8	19.466	13.408
14	Before splitting	Normal	19.104	14.707
	Splitting bus 9	9→14 9′→4,7,10, L	9.918	6.984
	Splitting bus 13	13→14 13′→12,6, L	11.8	8.776
13	Before splitting	Normal	30.129	22.973
	Splitting bus 14	14→13 14′→9, L	25.253	19.677
	Splitting bus 12	12→13 12′→6, L	26.785	20.724
	Splitting bus 6	6→13 6′→5,11,12, G, L	14.42	10.64
12	Before splitting	Normal	19.823	16.465
	Splitting bus 6	6→12 6′→5,11,13, G, L	10.413	8.661
	Splitting bus 13	13→12 13′→6,14, L	13.003	11.119
1	Before splitting	Normal	15.815	12.687
	Splitting bus 2	2→1 2′→3,4,5, G, L	9.861	8.497
	Splitting bus 5	5→1 5′→2,4,6, L	14.185	11.699
2	Before splitting	Normal	19.195	14.036
	Splitting bus 1	1→2 1′→5, G	15.128	10.95
	Splitting bus 3	3→2 3′→4, L, G	16.768	12.693
	Splitting bus 4	4→2 4′→7,9,5,3, L	17.685	13.303
		4→2,5 4′→7,9,,3, L	16.792	12.937
	Splitting bus 5	5→2 5′→1,4,6, L	17.963	13.392

Table 2 (continued)

Faulty bus	Network configuration	Splitting scenarios	Max. fault current (kA)	Min. fault current (kA)
3	Before splitting	Normal	16.260	10.15
	Splitting bus 4	4→3 4′→2,5,7,9,L	13.597	8.077
	Splitting bus 2	2→3 2′→1,4,5, G, L	13.642	7.997
4	Before SPLITTING	Normal	15.567	10.825
	Splitting bus 2	2→4 2′→ 1,3,5, G, L	13.601	9.44
		2→4,5 2′→1,3, G, L	12.246	8.404
	Splitting bus 3	3→4 3′→2, L, G	12.825	9.031
	Splitting bus 5	5→4 5′→1,2, 6, L	11.969	8.23
5	Before splitting	Normal	13.361	10.133
	Splitting bus 1	1→5 1′→2. G	11.481	8.738
	Splitting bus 2	2→5 2′→1,3,4, G, L	11.242	8.658
		2→4,5 2′→1,3,G,L	10.516	7.871
	Splitting bus 4	4→5 4′→2,3,7,9, L	7.566	6.555
6	Before splitting	Normal	60.274	43.293
	Splitting bus 11	11→6 11′→10, L	54.965	40.422
	Splitting bus 12	12→6 12′→13, L	59.596	43.244
	Splitting bus 13	13→ 6 13′→ 12,14, L	57.132	42.754
		13→6,12 13′→14, L	54.583	41.641

5.1.2 Relay co-ordination in IEEE 14-bus system with busbar splitting

The same case is considered as that for MBPS-based relay co-ordination, i.e., a fault occurs at busbar 11. The splitting scheme of busbar 11 is presented in Fig. 6, and the fault currents seen by each relay are given in Table 3 after splitting. It can be seen that after the busbar splitting, relays R14 and R15 do not see any fault current, and the section of the network starting from busbar 11 becomes radial. This takes the concept of MBPS out of consideration with the nearest relay, i.e., relay R1, being the primary relay and the starting point for relay co-ordination. It is assumed that the initial setting of relay R1 is TMS = 0.025 and the CTI for relay co-ordination is 0.3 s. For relay R1, before busbar splitting,

$$\left(I_{FMAX}/I_S\right) = \left(\frac{7.073KA}{\frac{2}{3} \times 6.83KA}\right) = 1.553$$

and after splitting of busbar 11,

$$\left(I_{FMAX}/I_S\right) = \left(\frac{10.3KA}{\frac{2}{3} \times 8.462KA}\right) = 1.825$$

Table 4 shows the TMS and t_{op} of the relay nearest to a fault and also of their backup relay, while Table 5 depicts the TMS and t_{op} for each relay after the busbar splitting, with the blank places indicating no fault current for the corresponding relays. From Tables 1 and 4, it is deduced that the time of operation, t_{op}, of the relay nearest to the fault, i.e., relay R1, has reduced from 1.5943 s (before splitting) to 0.4169 s (after splitting). Also, t_{op} for the

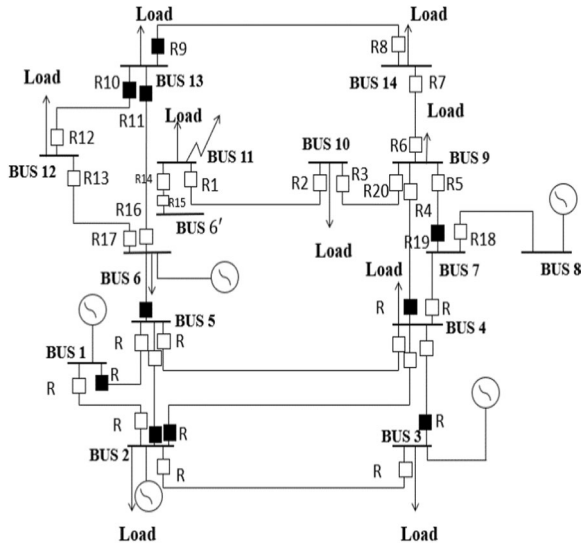

Fig. 6 IEEE 14-bus system with busbar splitting

Table 3 Minimum and maximum fault current observed by each relay in the IEEE 14-bus sytem

Relay	After busbar splitting		Before busbar splitting	
	I_{FMAX}(kA)	I_{FMIN}(kA)	I_{FMAX}(kA)	I_{FMIN}(kA)
R1	10.3	8.462	7.073	6.83
R2	10.3	8.462	7.073	6.83
R3	10.3	8.462	7.073	6.83
R4	0	0	0	0
R5	7.854	6.453	6.01	5.799
R6	2.631	2.162	1.135	1.095
R7	2.631	2.162	1.135	1.095
R8	2.631	2.162	1.135	1.095
R9	2.631	2.162	1.135	1.095
R10	0.538	0.442	0.232	0.224
R11	2.101	1.726	0.906	0.874
R12	0.538	0.442	0.232	0.224
R13	0.538	0.442	0.232	0.224
R14	0	0	13.652	13.172
R15	0	0	13.652	13.172
R16	2.101	1.726	0.906	0.874
R17	0.538	0.442	0.232	0.224
R18	7.854	6.453	6.01	5.799
R19	7.854	6.453	6.01	5.799
R20	10.3	8.462	7.073	6.83

back-up relay R1 has reduced from 1.846 s (before splitting) to 0.7169 s (after splitting). This shows that, after splitting, (I_{FMAX}/I_s) increases and thus leads to a reduction in t_{op} as in (1). Figure 7 shows the flowchart for relay co-ordination with busbar splitting approach.

Table 4 TMS and t_{op} of relay nearest to fault and the back-up relay (after splitting) in the IEEE 14-bus system

Faulty bus	Relay nearest to fault	t_{op} of nearest relay (s)	Back-up of nearest relay	t_{op} of backup relay (s)
11	R1	0.4169	R3	0.7169
	R14	0	–	–

Figure 7 shows the flowchart for the relay co-ordination with busbar splitting approach.

5.2 Relay co-ordination in IEEE 30-bus system with MBPS

A similar analysis has been done for the IEEE 30-bus system using the proposed method, and Fig. 8 shows the breakpoints of the IEEE 30-bus system (darkened relays). In this case, a LLL fault is considered at bus 17 and the fault current values shown in Table 6 are obtained from the simulation in ETAP. The TMS and t_{op} for the required relays (R4 and R7 for fault at bus 17) are calculated using (1) with the initial assumptions of TMS = 0.025 for the breakpoint relays and CTI of 0.3 s. Table 7 shows the TMS and the t_{op} of the relays nearest to the fault location. It can be seen that, in a normal scenario, i.e., without busbar splitting, the respective TMS and t_{op} for relay R4 are 0.1011 and 1.204 s, and 0.03 and 0.378 s for relay R7.

5.2.1 Relay co-ordination in IEEE 30-bus system with busbar splitting

For the fault at bus 17, the boundary bus 10 is split such that the net fault current at bus 17 can be reduced. Figure 9 shows that bus 10 is split into bus 10 and 10′ respectively. Such a splitting results in reducing the maximum fault current at bus 17 from 15.579 to 14.957 kA and the minimum fault current from 13.331 kA to 12.866 kA (as can be seen in Table 6). Splitting of bus 10 also converts the part of the system containing bus 17 into radial form. Thus, the starting relay for co-ordination is the relay nearest to the fault rather than the breakpoint relays, i.e., relay R4. In addition, relay R7 doesn't see any fault current, and hence the TMS and t_{op} for relay R7 have no value as can be seen in Table 7. The TMS and t_{op} for R4 are found to be 0.025 and 0.312 s, as shown in Table 7. It can be seen that, t_{op} has reduced from 1.204 s under conventional method to 0.312 s when the busbar splitting scheme is incorporated.

5.2.2 Relay co-ordination in IEEE 30-bus system with MBPS for multiple faults

In this case, faults are considered at buses 17 and 23, i.e., at multiple locations, as shown in Fig. 10. For the case of

Table 5 TMS and t_{op} of all relays before and after splitting in the IEEE 14-bus system

Relay No	Faulty Bus	TMS (after busbar splitting)	Operating time of relay (t_{op} (s)) after splitting	TMS (with MBPS considered)	Operating time of relay (t_{op} (s)) before splitting
R1	Bus 11	0.025	0.4169	0.1007	1.5943
R2		–	–	0.0819	1.2959
R3		0.0429	0.7169	0.0818	1.2943
R4		0.0609	–	0.1198	–
R5		0.0609	1.0171	0.1198	1.8923
R6		0.0609	1.0169	0.0628	0.9932
R7		–	–	0.1198	1.8917
R8		0.0789	1.3169	0.0439	0.6932
R9		–	–	0.025	0.3946
R10		0.0969	1.6209	0.025	0.4692
R11		0.0969	1.6176	0.025	0.3946
R12		–	–	0.0439	0.6946
R13		0.114	1.9209	0.0409	0.7692
R14		–	–	0.063	0.99501
R15		–	–	0.1180	1.846
R16		–	–	0.0439	0.693
R17		–	–	0.0628	0.9946
R18		0.0609	1.0160	0.1943	2.1923
R19		–	–	0.12	1.8954
R20		–	–	0.1008	1.5959

Table 6 Fault current at faulty buses before and after splitting in IEEE 30-bus system

Faulty bus	Before busbar splitting		After busbar splitting	
	Max. fault current (kA)	Min. fault current (kA)	Max. fault current (kA)	Min. fault current (kA)
17	15.579	13.331	14.957	12.866
17 and 23	At bus 17: 15.579 At bus 23: 15.461	At bus 17: 13.331 At bus 23: 13.244	At bus 17: 14.957 At bus 23: 14.85	At bus 17: 12.865 At bus 23: 12.787

relay co-ordination with MBPS, the maximum and minimum fault currents seen at buses 17 and 23 are given in Table 6. Table 8 provides the TMS and t_{op} of the relays nearest to the fault (before splitting cases), which have been calculated using (1) with an initial assumption of TMS = 0.025 for breakpoint relays and CTI of 0.3 s.

5.2.3 Relay co-ordination in IEEE 30 bus system with bus bar splitting for multiple faults

For multiple faults, bus bar splitting is considered for each fault location. In this case, bus 17 and bus 23 are under fault, and bus 10 and bus 15 are split as shown in Fig. 11. This results in reduced fault currents as can be seen in Table 6.

With the splitting of bus 10 into bus 10 and 10′, and bus 15 into bus 15 and 15′, the buses under fault are no longer part of any loop. This leads to the nearest relay being the starting point for relay co-ordination. As can be seen in Table 8, after splitting of busbars the t_{op} for relay R4 has reduced from 1.204 s (before splitting) to 0.312 s and for relay R14, it is reduced from 1.52 s (before splitting) to 0.313 s. Also, relays R7 and R11 do not see any fault current.

6 Conclusion

An adaptive relay co-ordination scheme is mainly focused on reducing the operating time of the relays based on the busbar splitting scheme applicable for SIPS. The scheme is based upon the short-circuit level of the network. Relay co-ordination is tested for the IEEE14-bus and 30-bus systems considering different scenarios such as single LG fault, single LLL fault, and multiple LLL faults. The

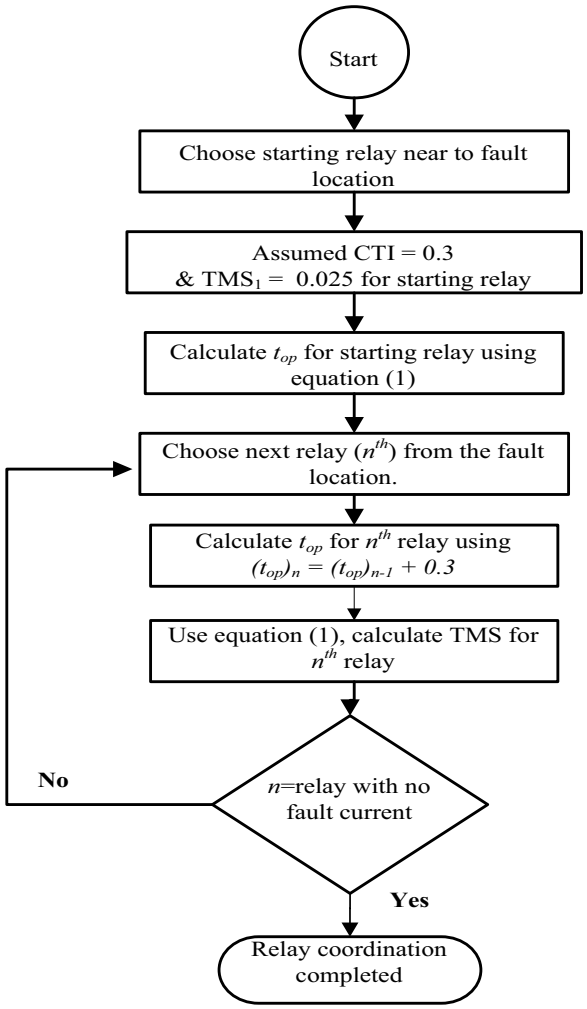

Fig. 7 Flowchart for relay co-ordination with busbar splitting

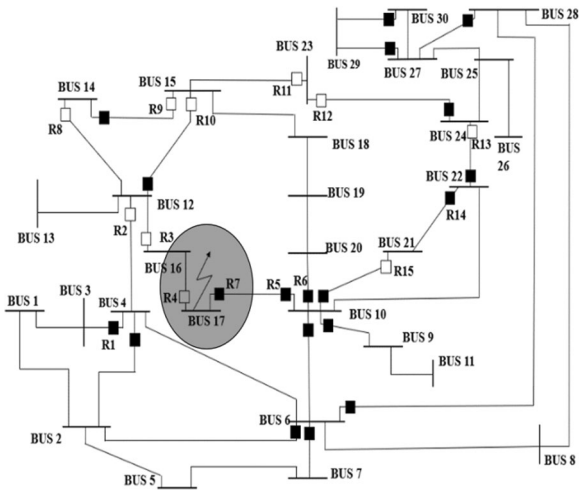

Fig. 8 IEEE 30-bus system with breakpoints and fault at bus 17

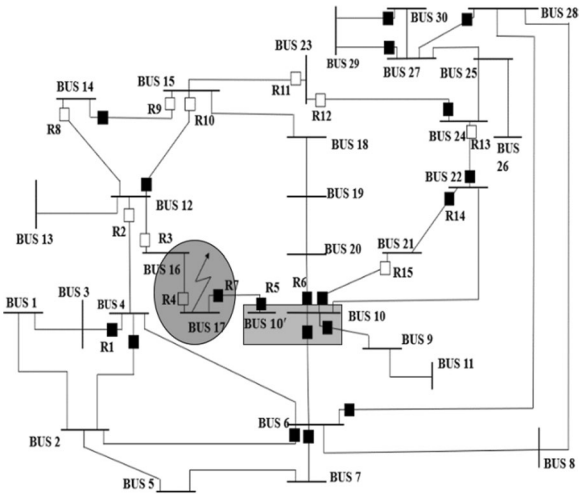

Fig. 9 IEEE 30-bus system with single fault and busbar splitting scheme incorporated

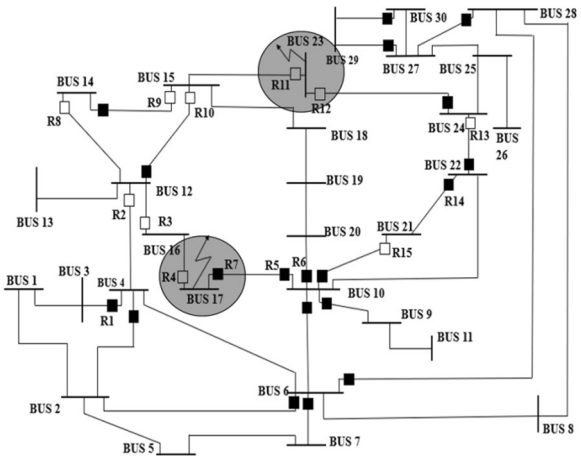

Fig. 10 IEEE 30-bus system under multiple fault locations

Table 7 TMS and t_{op} of relays nearest to fault location

Faulty bus	Relay nearest to fault	TMS (before busbar splitting)	t_{op} of nearest relay (before splitting) (s)	TMS (after busbar splitting)	t_{op} of nearest relay (after splitting) (s)
17	R4	0.1011	1.204	0.025	0.312
	R7	0.030	0.378	–	–

proposed scheme significantly reduces the relay operating time and minimises the dependency on MBPS identification. Also, the proposed relay co-ordination technique will not be affected with small scale distributed

Table 8 TMS and t_{op} of relays nearest to fault location (before and after splitting) considering multiple faults in the IEEE 30-bus system

Faulty bus	Relay nearest to fault	TMS (before busbar splitting)	t_{op} of nearest relay (before splitting) (s)	TMS (after busbar splitting)	t_{op} of nearest relay (after splitting) (s)
17	R4	0.1011	1.204	0.025	0.312
	R7	0.030	0.378	–	–
23	R11	0.123	1.495	–	–
	R14	0.118	1.52	0.025	0.313

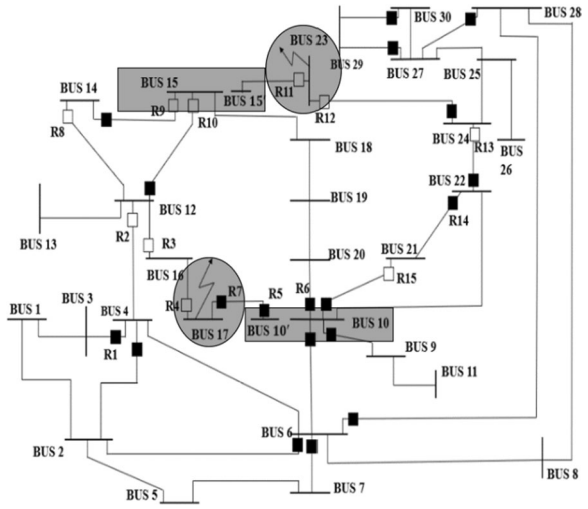

Fig. 11 IEEE 30-bus system under multiple faults and busbar splitting incorporated

generation integration in the sub-transmission level of the power system network. However, incorporation of large-scale distributed generation changes the short-circuit current and the power flow directions to bi-directional over conventional power flow. Thus, the proposed busbar splitting based relay co-ordination applicable for networks with large scale distribution generation integration having bi-directional power flow feature may be considered as a potential area for future work.

List of symbols

t_{op}: Relay operating time; *TMS*: Time multiplier setting; I_{FMAX}: Maximum fault current; I_{FMIN}: Minimum fault current; I_S: Pick-up current of relay; Z_{ab}: Impedance between buses *a* and *b*; Z_n: Impedance between bus *n* and neutral; *P*: Bus under consideration for elimination; *Q*: Boundary buses of bus *P*; *R*: External buses of bus *P*; Y_{XX}: Self admittance matrix of bus *X*; Y_{XY}: Mutual admittance matrix between buses X and Y; $\widehat{Y_{QQ}}$: Reduced equivalent boundary bus admittance matrix before busbar spitting; $\widehat{Z_{QQ}}$: Reduced equivalent boundary bus impedance matrix before busbar splitting; $\widehat{Z_{QQ}}^*$: Reduced equivalent boundary bus impedance matrix after busbar splitting; $\widehat{Y_{QQ}}^*$: Reduced equivalent boundary bus admittance matrix before busbar splitting.

Acknowledgements
Not applicable.

Authors' contributions
RS proposed the adaptive relay coordination method and implemented the same on a test system. NKR contributed to enhancement of the simulation modelling for modified analysis of results. DG contributed for results verification and guide for the necessary modifications in the proposed method. All authors read and approved the final manuscript.

Funding
Not applicable.

Availability of data and materials
Not applicable.

Declarations

Competing interests
The authors declare that they have no known competing financial interests or personal relationships that could have appeared to influence the work reported in this paper.

Received: 17 August 2020 Accepted: 23 March 2022
Published online: 06 April 2022

References

1. Begovic, M., Madani, V., & Novosel, D. (2007, August). System integrity protection schemes (SIPS). In *2007 iREP symposium-bulk power system dynamics and control-VII. Revitalizing operational reliability* (pp. 1–6). IEEE.
2. Rajalwal, N. K., & Ghosh, D. (2020). Recent trends in integrity protection of power system: A literature review. *International Transactions on Electrical Energy Systems, 30*(10), e12523.
3. Kundu, P., & Pradhan, A. K. (2015). Enhanced protection security using the system integrity protection scheme (SIPS). *IEEE Transactions on Power Delivery, 31*(1), 228–235.
4. Yang, J. S., Liao, C. J., Wang, Y. F., Chu, C. C., Lee, S. H., & Lin, Y. J. (2017). Design and deployment of special protection system for Kinmen power system in Taiwan. *IEEE Transactions on Industry Applications, 53*(5), 4176–4185.
5. Wang, L., Howell, F., & Morison, K. (2008). A framework for special protection system modeling for dynamic security assessment of power systems. In *Joint international conference on power system technology and IEEE power India conference, New Delhi, India.*
6. Kundu, P., & Pradhan, A. K. (2018). Real-time analysis of power system protection schemes using synchronized data. *IEEE Transactions on Industrial Informatics, 14*(9), 3831–3839.
7. Nayak, P. K., Pradhan, A. K., & Bajpai, P. (2014). Wide-area measurement-based backup protection for power network with series compensation. *IEEE Transactions on Power Delivery, 29*(4), 1970–1977.
8. Kundu, P., & Pradhan, A. K. (2015). Online identification of protection element failure using wide area measurements. *IET Generation, Transmission & Distribution, 9*(2), 115–123.
9. Ravikumar, K. G., & Srivastava, A. K. (2019). Designing centralised and distributed system integrity protection schemes for enhanced electric grid resiliency. *IET Generation, Transmission & Distribution, 13*(8), 1194–1203.

10. Gawande, P., & Dambhare, S. (2019). New predictive analytic-aided response-based system integrity protection scheme. *IET Generation, Transmission & Distribution, 13*(8), 1204–1211.
11. Ananthan, S. N., & Santoso, S. (2019). Universal model-based fault location for improved system integrity. *IET Generation, Transmission & Distribution, 13*(8), 1212–1219.
12. Beheshtaein, S., Cuzner, R., Savaghebi, M., Golestan, S., & Guerrero, J. M. (2019). Fault location in microgrids: A communication-based high-frequency impedance approach. *IET Generation, Transmission & Distribution, 13*(8), 1229–1237.
13. Samantaray, S. R., & Sharma, A. (2019). Supervising zone-3 operation of the distance relay using synchronised phasor measurements. *IET Generation, Transmission & Distribution, 13*(8), 1238–1246.
14. Das, S., & Panigrahi, B. K. (2019). Prediction and control of transient stability using system integrity protection schemes. *IET Generation, Transmission & Distribution, 13*(8), 1247–1254.
15. Nadkarni, A., & Soman, S. A. (2019). Real-time spatio-temporal trend and level (T&L) filtering scheme for early detection of voltage instability. *IET Generation, Transmission & Distribution, 13*(8), 1255–1265.
16. Liu, L., & Fu, L. (2016). Minimum breakpoint set determination for directional overcurrent relay coordination in large-scale power networks via matrix computations. *IEEE Transactions on Power Delivery, 32*(4), 1784–1789.
17. National Programme on Technology Enhanced Learning. Retrieved June 2, 2020, from.https://nptel.ac.in/content/storage2/courses/108101039/download/Lecture-19.pdf
18. Gajbhiye, R. K., De, A., & Soman, S. A. (2007). Computation of optimal break point set of relays: An integer linear programming approach. *IEEE Transactions on Power Delivery, 22*(4), 2087–2098.
19. Vinnakota, B. R. V., & Ababei, C. (2011). Determination of the minimum breakpoint set of directional relay networks based on k-trees of the network graphs. *IEEE Transactions on Power Delivery, 26*(4), 2318–2323.
20. Ustariz-Farfan, A. J., Cano-Plata, E. A., & Arias-Guzman, S. (2019). Identification of protection coordination break points: A power quality approach. *IEEE Industry Applications Magazine, 25*(5), 68–82.
21. Dolatabadi, M., & Damchi, Y. (2019). Graph theory based heuristic approach for minimum break point set determination in large scale power systems. *IEEE Transactions on Power Delivery, 34*(3), 963–970.
22. Kovalsky, L., Yuan, X., Tekletsadik, K., Keri, A., Bock, J., & Breuer, F. (2005). Applications of superconducting fault current limiters in electric power transmission systems. *IEEE Transactions on Applied Superconductivity, 15*(2), 2130–2133.
23. Sugimoto, S., Kida, J., Arita, H., Fukui, C., & Yamagiwa, T. (1996). Principle and characteristics of a fault current limiter with series compensation. *IEEE Transactions on Power delivery, 11*(2), 842–847.
24. Sun, M., Lin, Y., & Guo, Y. (2011, May). The study of power system performances in the fast short circuit current limiter embedded network. In *2011 10th international conference on environment and electrical engineering* (pp. 1–4). IEEE.
25. Hartung, K. H., & Schmidt, V. (2009, September). Limitation of short circuit current by an I S-limiter. In *2009 10th international conference on electrical power quality and utilisation* (pp. 1–4). IEEE.
26. Abramovitz, A., & Smedley, M. (2012). Survey of solid-state fault current limiters. *IEEE Transactions on Power Electronics, 27*(6), 2770–2782.
27. Ward, J. B. (1949). Equivalent circuits for power-flow studies. *Electrical Engineering, 68*(9), 794–794.
28. Shi, Di. (2012). *Power system reduction for engineering and economic analysis*. Arizona State University.
29. Wang, L., & Chiang, H. D. (2016). Toward online bus-bar splitting for increasing load margins to static stability limit. *IEEE Transactions on Power Systems, 32*(5), 3715–3725.
30. Trodden, P. A., Bukhsh, W. A., Grothey, A., & McKinnon, K. I. M. (2012, July). MILP islanding of power networks by bus splitting. In *2012 IEEE power and energy society general meeting* (pp. 1–8). IEEE.
31. Shao, W., & Vittal, V. (2004, October). A new algorithm for relieving overloads and voltage violations by transmission line and bus-bar switching. In *IEEE PES power systems conference and exposition, 2004* (pp. 322–327). IEEE.
32. Namchoat, S., & Hoonchareon, N. (2013, May). Optimal bus splitting for short-circuit current limitation in metropolitan area. In *2013 10th international conference on electrical engineering/electronics, computer, telecommunications and information technology* (pp. 1–5). IEEE.
33. Wu, X., Mutale, J., Jenkins, N., & Strbac, G. (2003). An investigation of network splitting for fault level reduction. *The Manchester Centre for Electrical Energy (MCEE), UMIST, UK*.
34. Pati, R. S., & Ghosh, D. (2020, June). Busbar splitting approach for fault level management for system integrity protection scheme. In *2020 First IEEE international conference on measurement, instrumentation, control and automation (ICMICA)* (pp. 1–4). IEEE.